GNSS PEST CONTROL

Correlator Beamforming for Low-Cost Multipath Mitigation

By Sanjeev Gunawardena, John Raquet and Mark Carroll

Multipath is the single largest naturally occurring un-modeled error source that affects high-accuracy and differential GNSS applications. Even though decades of research and development on advanced multipath mitigating antennas and correlator-gating techniques have contributed significantly to reducing the effects of this error source, short delay, higher elevation-angle and carrier multipath continue to be a problem. It is well known that antenna array-based beamforming is particularly effective against these types of multipath. However, traditional antenna array and related beamforming processing technology is large, heavy, power-hungry and costly in many applications.

A new alternative solution called correlator beamforming employs simple radio-frequency (RF) signal switching and a single front end to reduce complexity, power consumption and cost. This technology is privately patented and is already commercially available in devices that run in the 2.4 GHz industrial, scientific and medical (ISM) frequency band. These systems have been leveraged into heavy industrial environments where precision position, navigation and time (PNT) is critically important to drive operations, especially for a large number of vehicle and fleet automation systems under development. These new unmanned aerial vehicle (UAV), machine automation and fleet management systems must have a level of continuous reliability, which cannot be guaranteed by satellite-based systems in difficult, high-multipath environments such as mines, ports, warehouses and urban canyons. Correlator beamforming has been shown to be effective at mitigating multipath for these non-GNSS terrestrial and challenging indoor applications.

Intrigued by the technology's demonstrated accuracy in multipath-plagued environments, the Air Force Institute of Technology's (AFIT's) Autonomy and Navigation Technology (ANT) Center initiated a collaborative research and development agreement (CRADA) with Locata Corporation to investigate the feasibility of applying the correlator beamforming techniques to standard GNSS. The AFIT results show that a GPS receiver employing correlator beamforming technology is nearly as effective as a traditional beamforming receiver at rejecting multipath.

BACKGROUND

Often considered the bane of precision navigation for indoor or urban applications using RF signals, multipath continues to be one of the major error sources of GNSS. The presence of reflected signals in these environments often degrades the accuracy and reliability of such PNT systems, a problem that GPS engineers have struggled with since GPS signals were first broadcast. Fortunately, the industry has been able to implement multipath mitigation approaches, albeit with varying levels of success and technical tradeoffs. Nevertheless, there is a clear understanding today that future autonomous, mobile and personal applications require a level of accuracy and reliability that demand better multipath mitigation solutions.

There are two prevalent techniques, apart from modern GNSS signal structures that have anti-multipath features by design, that are used to mitigate multipath: antenna gain pattern shaping and receiver correlator gating. The first technique limits the effect of ground multipath by reducing antenna gain at low elevation

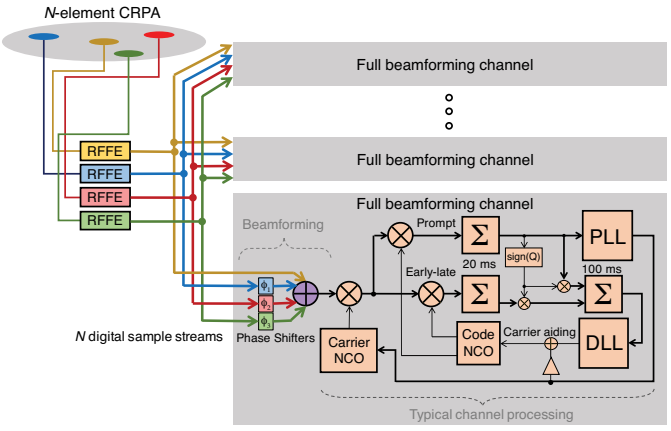

FIGURE 1 Traditional beamforming receiver architecture.

INNOVATION INSIGHTS

BY RICHARD B. LANGLEY

WHICH IS MORE IMPORTANT for GNSS equipment: the antenna or the receiver? Of course, answering this question is a mug's game as both are vitally important and one is useless without the other. It is true that the development of sensitive receivers has permitted the use of inexpensive linearly polarized wire or chip antennas in consumer electronics such as mobile phones. But demanding applications such as geodetic surveying, timing and machine control require a "proper" right-hand-circularly-polarized antenna. However, regardless of the application — whether low accuracy or high — the antenna must be omnidirectional. So GNSS antennas typically have a broad gain pattern allowing reception of signals arriving at any azimuth and elevation angle. Many simple antennas, such as a microstrip patch on a small ground plane, may even have significant sensitivity to signals arriving from below, that is, ground-bounce multipath. The multipath signals, whether coming from the ground or nearby structures, once passed to the receiver, interfere with the direct line-of-sight signals and can be a real pest, degrading the pseudorange and carrier-phase measurements and limiting the resulting position, velocity and timing accuracy of the equipment.

Advanced correlator techniques and clever broad-pattern antenna designs can mitigate some forms of multipath. The multipath-estimating delay-lock loop is an example of the former, while the choke-ring antenna and the novel antenna design discussed in this column a few months ago are examples of the latter. Ideally, a GNSS antenna should only receive line-of-sight signals from the satellites (except for some scientific applications like snow-depth monitoring or water-level measurement or when some line-of-sight signals are blocked such as in concrete canyons and a reflected signal is better than nothing). That could be arranged by using a narrow beam antenna such as a small parabolic dish. In fact, such an antenna was used by the Jet Propulsion Laboratory for one of the first codeless GPS receivers. Called SERIES, for Satellite Emission Range Inferred Earth Surveying, it used a 1.5-meter-diameter dish antenna mounted on a trailer. It would cycle through the visible satellites, repointing the dish and spending several minutes on each satellite to determine the antenna's position. Additionally, by using a pair of terminals and taking data over an hour or so, the baseline between the terminals could be determined to a few centimeters.

SERIES was an outgrowth of JPL's work in very long baseline interferometry. In interferometry, a very narrow antenna beam is synthesized by combining the measurements made by the two (or more) antennas and receivers. The beam width is proportional to the wavelength of the received signals and inversely proportional to the baseline length. While VLBI observations of quasars and other esoteric celestial objects have provided some of our best knowledge of plate tectonics and the Earth's rotation and establish the link between the terrestrial and celestial reference frames, interferometry using slewing dishes was not a practical approach for GPS positioning, and JPL moved to more conventional antennas for its SERIES receivers. JPL's use of interferometry for GPS positioning (also pioneered by the Massachusetts Institute of Technology with its Macrometer receiver) led to the common carrier-phase double-differencing technique widely used today for high accuracy GNSS positioning.

But the concept of a narrow antenna beam for GNSS signal reception would be practical if the beam could be rapidly directed in sequence towards each of the visible satellites. This could be done with a pair of adjacent antenna elements by adjusting (under software control) the relative phase of the signals provided by each element. A more efficient approach would be to use multiple elements. Such beamforming antennas have actually been constructed and are commercially available. Not only do these antennas provide enhanced multipath rejection, they can be configured to produce a null in the combined gain pattern in the direction of an interference source — an important antenna characteristic for military applications.

As you might expect, these beamforming antennas and their associated electronics are large and heavy and consume a fair bit of power and so are not well-suited for general purpose positioning. However, a novel approach to beamforming without these shortcomings, and which was commercially developed for use in the 2.4-GHz band, has been adapted for GNSS use. In this month's column, a team of researchers at the U.S Air Force Institute of Technology discuss how they implemented the approach, termed correlator beamforming, and tested it with live GPS signals with excellent results.

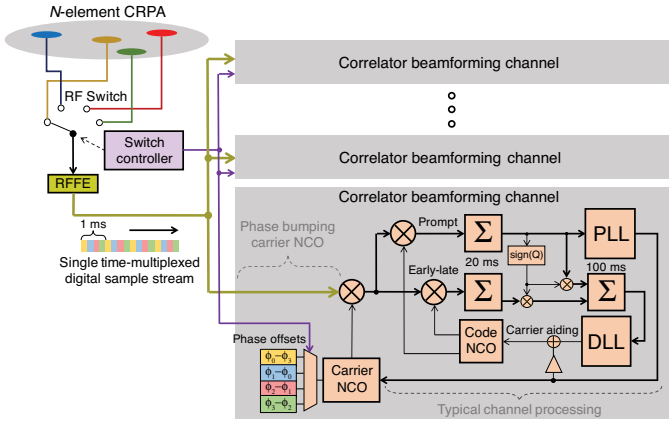

FIGURE 2 Correlator beamforming receiver architecture.

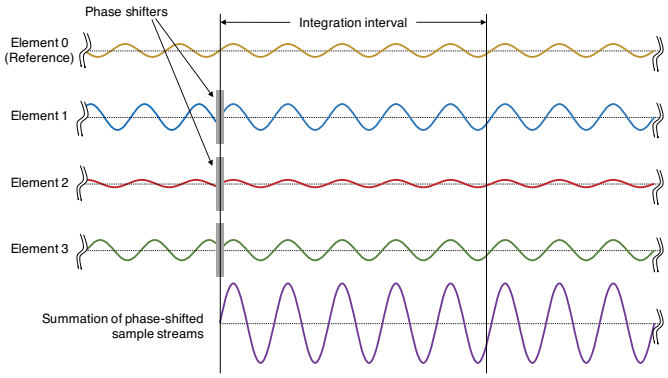

FIGURE 3 Simplified illustration of traditional beamforming for four sample streams.

angles. This comes at the expense of reducing the number of satellites available for a position solution, which results in increased dilution of precision. Antenna gain shaping provides no defense against multipath from higher elevation angles, such as that experienced in urban environments.

The second common approach uses correlator gating, which exploits the generally valid assumption that the direct signal always precedes a reflected one. Hence, correlators used for code tracking are gated such that timing information is extracted from as close to the underlying direct signal's phase transitions as possible. This technique comes at the expense of reduced code-tracking sensitivity and robustness. The need for wide front-end bandwidth to differentiate the direct signal from multipath generally increases the overall power consumption of the receiver. Hence, the use of advanced gated correlator techniques becomes less attractive for portable and consumer-level applications. Moreover, the achievable short-delay code multipath performance of correlator gating is limited by theoretical lower bounds.

Other techniques used to mitigate multipath involve directive antennas and spatial diversity. Highly directive antennas such as parabolic dishes have limited utility except in high-fidelity per-satellite signal monitoring applications. And spatial diversity techniques based on antenna motion such as the use of rotating antennas are practical only for stationary or low-user-dynamics applications.

One powerful multipath mitigation technology commonly used today is called the controlled reception pattern antenna (CRPA), which employs a large multi-element antenna array. Although developed primarily as an anti-jam system for critical military GNSS applications, these complex antennas, and the associated electronics packages required to produce beamforming, provide both code and carrier multipath rejection when individual beams are formed towards satellites. This lessens the impact of multipath signals coming from other directions. **FIGURE 1** illustrates a typical architecture for a traditional beamforming CRPA system.

For each satellite tracking channel, the digitized sample streams from individual antenna elements are time shifted and summed such that the desired signal powers received by each element coherently add. Ideally, this results in an N^2 increase in signal power for N elements. Consequently, the uncorrelated noise powers from each sample stream also add to yield an N-fold increase in noise power. The net result is an N-fold increase in signal-to-noise-density ratio (S/N_0). In the spatial domain, this time shifting and summation process to maximize received signal power corresponds to forming a beam in the direction of arrival of a particular signal. Any time-correlated signals incident on the CRPA from other directions will generally combine incoherently as they pass through this beamforming process. These other signals may include other GNSS signals, interference (both narrow and wideband) and multipath. The digital delays — and the amplitudes of the streams — can be adjusted such that these unwanted signals can be made to cancel according to a given optimization criterion. This describes the essence of forming one or more nulls in particular directions.

Adopting traditional beamforming technology for high- or medium-volume applications remains elusive primarily due to the costs and complexities associated with needing an individual RF front end for each antenna element. The greatly increased power consumption associated with having to process multiple

streams of data, along with the size and weight of the complex electronics required to process the antenna's received signals, are significant issues for portable or consumer-level applications.

Unlike conventional or traditional beamforming technology, the new correlator beamforming approach combines RF signals received by any number of individual antenna elements into a single switched-RF signal. This time-multiplexed signal is then downconverted and digitized by a single RF front-end. The correlator beamforming design should offer manufacturing cost savings because the resulting data stream is processed using a single correlator channel per beam. This reduces the complexity when compared to the traditional beamforming methodology. The architectural differences between a standard single-antenna setup, a traditional beamforming CRPA system, and correlator beamforming are shown in Figure 1 and **FIGURE 2.**

CORRELATOR BEAMFORMING

The correlator beamforming technique performs antenna array signal processing to form beams as part of a receiver's correlation process. The complete explanation of this technology can quickly get complex, even for the seasoned RF engineer. To describe this process more simply, we will assume noiseless signals and no multipath (except as noted), as well as equal noise figures for all front-end processing chains. To further simplify our explanation, modulation on the carrier and switching losses will be ignored.

FIGURE 3 illustrates traditional beamforming processing as applied to a four-element CRPA. The four sinusoids shown depict the baseband sampled signal carriers received by each element from a satellite at a particular azimuth and elevation angle with respect to the center element. Note that the phases of the signals for Elements 1 through 3 prior to the phase shifters are different from the reference Element 0. The reasons for these phase differences are twofold: (1) slightly different signal propagation distances from the satellite to each element's phase center as a function of array geometry and orientation, and (2) differences in the electrical path lengths from each element's phase center to the front-end analog-to-digital converter (ADC). The latter effects are a combination of angle-of-arrival (AoA) dependent and independent inter-channel biases and comprise what is normally referred to as the antenna manifold.

Note the unequal amplitudes of the received signals. This is intended to represent differences in the gain patterns of each individual antenna element as well as minor gain differences in the signal processing chains (amplifiers, filters, mixers, transmission lines and ADCs). In general, for beamforming applications (as opposed to null-forming) it is not necessary to compensate for these. Amplitude compensation at the sample level significantly increases the signal processing burden. Furthermore, in the context of this article, one or two bits of sample amplitude quantization is adequate for multipath rejection as long as no significant interference is expected.

As shown in Figure 3, phase shifts are applied such that all signals are phase aligned to the reference element. The coherent sample streams can then be summed to maximize received signal power. In the spatial domain, this corresponds to steering a beam in the direction of the desired signal. This visual interpretation arises from the fact that the specific set of phase shifts that aligns the signals coherently only applies to signals arriving from this desired signal's direction.

Under the conditions described above, if a multipath signal arrives from a different direction than that which is intended, the phase of the multipath signals in the four elements will not be coherent, so the multipath signal will not experience the same N^2 power gain as the direct signal. This is the fundamental reason that such a system rejects multipath signals — by steering the beam, the effective gain of the direct signal is higher than the effective gain of the multipath signals.

Even though not shown in Figure 3, it should be clear that the coherently combined sample stream undergoes typical GNSS receiver baseband processing (that is, correlation with a locally-generated replica, carrier/code

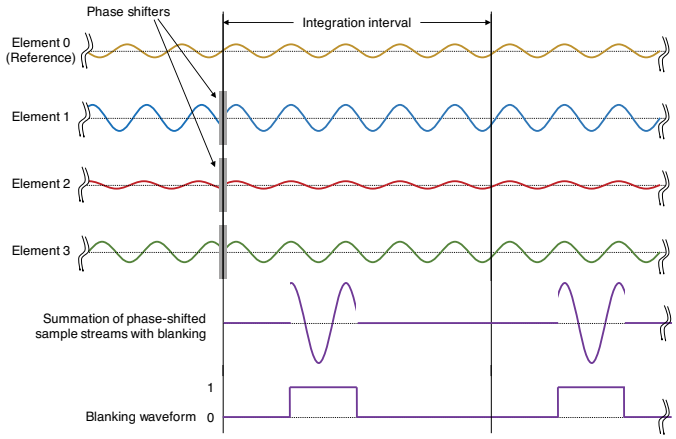

FIGURE 4 Illustration of traditional beamforming with 25 percent duty-cycling.

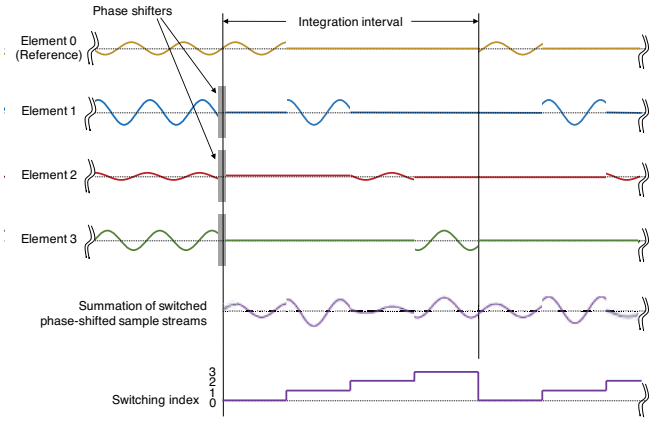

FIGURE 5 Illustration of 1/*N* duty-cycling replaced by *N*-to-1 switching.

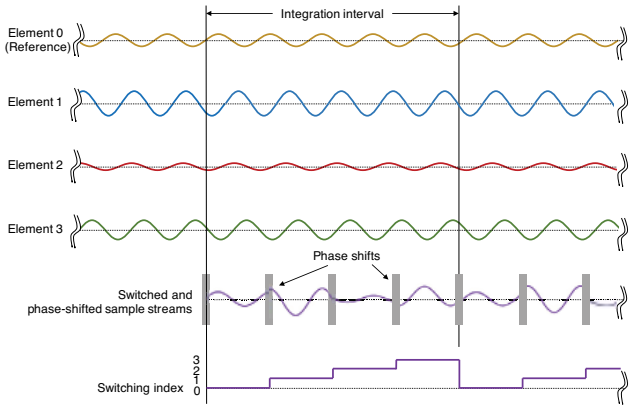

FIGURE 6 Illustration of *N*-to-1 switching with phase shifts applied at switch-state transitions.

tracking and the computation of range measurements). The pre-detection integration interval applicable to the tracking channel is illustrated in the figure. By parallelizing this beamforming process, multiple beams can be formed simultaneously for each tracking channel, as shown in Figure 1.

Next, consider 1/*N* duty cycling applied to the tracking channel described above, where *N* is the number of antenna elements. This can be implemented as sample gating, as illustrated in **FIGURE 4**. It should be clear that this duty cycling negates the *N*-fold S/N_0 advantage of traditional beamforming. In other words, in the absence of multipath, the carrier-to-noise-density ratio (C/N_0) measured by the duty-cycled tracking channel that has formed a beam towards the received signal will equal the mean C/N_0 values measured by *N* single-element tracking channels, each connected to the individual sample streams. However, it should be clear that the spatial gain pattern of the CRPA (specific to the set of phase shifts applied to the elements) is unaffected by the duty cycling process. This means that such a system would have the same multipath rejection properties of the non-duty cycled case, because the multipath is still attenuated relative to the direct signal.

Consider now the case where each phase-aligned sample stream is sequentially selected for 1/*N* of the integration interval, as illustrated in **FIGURE 5**. This is essentially identical to an *N*-to-1 switch connected to the input of the tracking channel. Clearly, since no coherent combination of sample streams is taking place, C/N_0 measured by this tracking channel will equal the mean C/N_0 values of the individual sample streams — the same as that for 1/*N* duty cycling as depicted in Figure 4.

Consider only a GNSS signal's carrier signal buried within the (uncorrelated) thermal noise. For the relatively short duration of an integration interval, the carrier signals within the phase-aligned sample streams can be assumed to be time invariant (that is, each given cycle is the same as the ones before and after it). Therefore, whether all *N* sample streams are summed over a 1/*N* integration interval (duty cycling) or integrating 1/*N* of each sample stream over the entire integration interval, the processing gain remains the same. Under the assumption of time invariance, the beam gain also remains unchanged. Therefore, it can be said that these two processes are equal. It is stressed that this equality holds true only for time-invariant signals. For example, the multipath rejection ability discussed previously is retained for *N*-to-1 switching. However, there is no rejection capability for non-time-invariant signals such as broadband noise.

Rather than performing phase alignment prior to *N*-to-1 switching, it could be built into the switching process itself. This is conceptually illustrated in **FIGURE 6**. It is clear that phase shifting can be applied to either the incoming sample stream or the local replica to yield the same result. Hence, the phase rotations illustrated in Figure 6 can also be implemented by adding appropriate phase offsets to the phase accumulation register of the tracking channel's carrier numerically controlled oscillator (NCO). This is also known as phase bumping the carrier NCO (illustrated in Figure 2). The two compelling advantages of NCO phase bumping over phase rotating the switched sample stream are: 1) the resolution of a phase offset that can be applied to the carrier NCO is $1/2^K$ cycles, where *K* represents the number of bits comprising the NCO phase register. Typically, *K* can range between 20 and 64 bits resulting

FIGURE 7 GAS-1 CRPA with 51-inch-diameter rolled-edge ground plane installed on the roof of the ANT Center.

in extremely fine phase bumping granularity; 2) the switched sample stream becomes the common input to many correlator channels, each capable of forming beams independently as part of its correlation processing, as shown in Figure 2.

Finally, the *N*-to-1 switching thus far described in the context of switching baseband sampled streams can be moved upstream to switch RF signals from the antenna elements instead. The switched-RF signal can then be downconverted and sampled using only a single RF front end. This results in an elegant and cost-effective beamforming architecture — albeit minus the *N*-fold S/N_0 advantage of traditional beamforming and the ability to reject broadband noise.

EXPERIMENT SETUP

To evaluate the performance of correlator beamforming as fairly as possible compared to traditional beamforming and single-element processing, AFIT set up its data collection such that all three approaches could be implemented in a software receiver. Additionally, a seven-element Naval Air Systems Command GPS Antenna System 1 (GAS-1) antenna was used for this experiment. The antenna was mounted on a 51-inch (130-centimeter) diameter rolled-edge ground plane provided to the ANT Center by the MITRE Corporation. **FIGURE 7** shows the antenna installation.

The GAS-1 CRPA is comprised of passive elements. Therefore, to ensure a low system noise figure, low-noise amplifiers (LNAs) were introduced before the attenuation of the long low-loss cables that send the received signals to the ANT Center lab. A two-pole dielectric filter centered at L1 with an approximate 3-dB bandwidth of 20 MHz was used in front of each LNA. This was done to prevent any strong out-of-band signals from potentially saturating the LNAs. Consequently, the noise figure of each feed was directly affected by the insertion loss of the filter. However, the overall system noise figure was estimated to be less than 2.5 dB. **FIGURE 8** shows the installation of filters and LNAs underneath the CRPA.

Each individual feed from the CRPA was connected to an Ohio University Transform-Domain Instrumentation GNSS Receiver (TRIGR) front-end module. These modules contain an RF monitor output port — essentially an active splitter output after the first stage of amplification within the module. Each monitor output was connected to the input ports of an 8-to-1 RF switch (Port 8 is terminated). This digitally controlled switch is an evaluation board for the Analog Devices HMC321 device with RF shielding material applied. The RF switch output was connected to an eighth TRIGR front-end module. All eight TRIGR modules were fed the same (1575.42 minus 70.0) MHz local oscillator (LO) signal that was used for downconversion to a 70-MHz intermediate frequency (IF). The IF outputs were connected to an eight-channel ADC. The LO and 56.32-MHz sampling clock phase-locked oscillators were referenced to a 10-MHz low phase-noise rubidium oscillator. **FIGURE 9** shows the front-end hardware.

The low-voltage differential signaling output interface

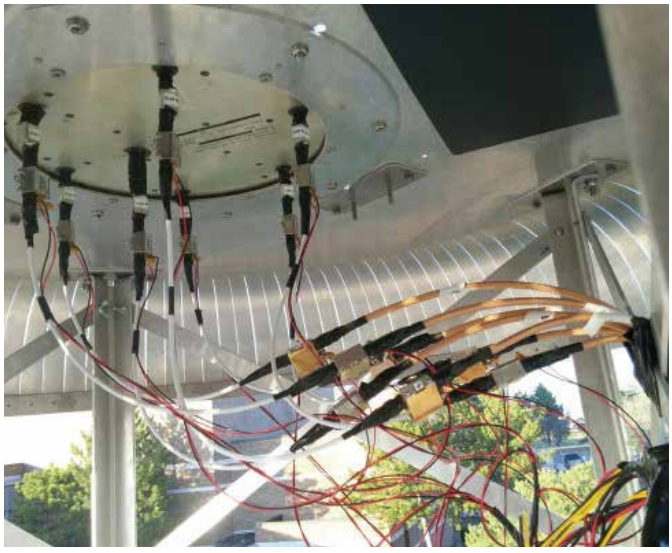

FIGURE 8 Underside of passive-element GAS-1 CRPA showing filters and LNAs used to ensure low system noise figure while driving long low-loss cables to the ANT Center.

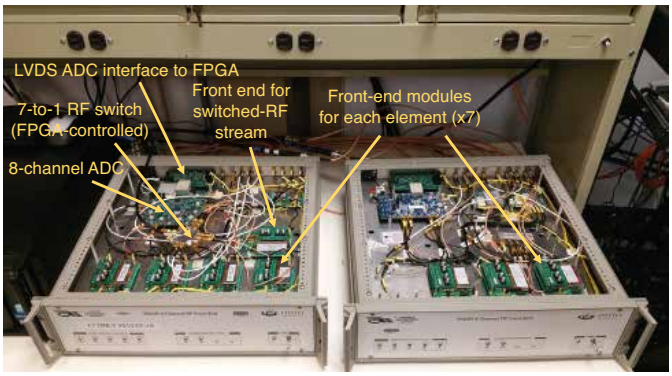

FIGURE 9 TRIGR front-end configuration. Eight front-end modules are used to downconvert and sample signals from the seven individual antenna elements and the switched-RF signal.

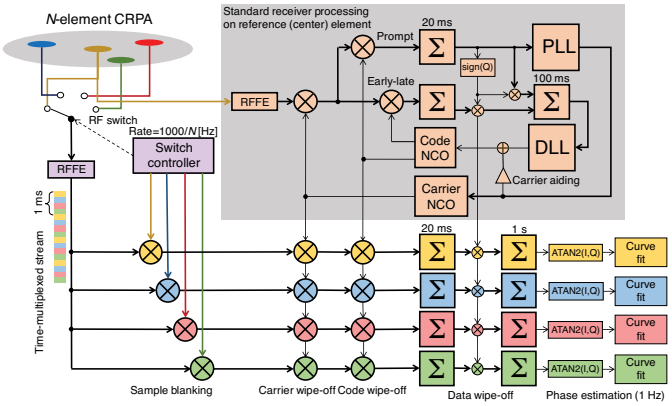

FIGURE 10 Illustration of procedure used to obtain phases relative to the reference element as a function of satellite PRN and time.

of the ADC was connected to a field-programmable gate array (FPGA). The design within the FPGA de-serializes the 12-bit samples from the ADC, reduces bit depth, and packs them into a 32-bit aligned datastream. For this experiment, a bit depth of 2 bits/sample was selected. This reduced the formatted stream data rate to approximately 113 megabytes per second. This data stream was continuously written to an array of hard disks. For this experiment, a 72-hour-long continuous data set was collected (approximately 29 terabytes).

The eight ADC sample streams packed into the formatted data stream described above was arranged in chunks, where the length of each chunk was 1 millisecond. The digital logic that generated these 1-millisecond intervals also generated the control signals for the RF switch. A delay compensation scheme was also implemented such that the switched samples from each of the seven elements were aligned to better than 1 sample (~18 nanoseconds) within a chunk.

The formatted data stream written to file contained eight sampled data streams. Streams 1 through 7 corresponded to the continuous signals from the individual CRPA elements. Stream 8 contained the time-multiplexed signals from Streams 1 through 7. With this data, software receiver processing can be performed to evaluate all three receiver architectures as fairly as possible.

However, it is important to note that for a final implementation of such a system, only the switched signal is required, which greatly reduces the hardware requirements from those used for this experiment.

Software receiver processing was performed for many tens of data hours to obtain the results presented in this article. To ensure reasonable runtimes, an efficient multi-threaded software correlation engine was used. This engine employs many of the same signal processing optimizations used in commercial GNSS receivers (such as fixed-point arithmetic). Furthermore, only algorithms realizable in real time were used. Therefore, it should be emphasized that the algorithms and results presented in this article are fully realizable in a real-time GNSS receiver.

ANTENNA ARRAY MANIFOLD MEASUREMENT

To form a beam to a specific AoA, the challenging task of estimating the array manifold must be performed first. Since the research reported here is focused on assessing multipath rejection performance and not general-purpose beamforming per se, a much simpler approach was used to estimate the required relative phase offsets.

Assuming no multipath, if a particular satellite signal is phase tracked on the reference element, then by definition the tracking channel's phase-locked loop (PLL) is phase aligning its replica carrier to that of the received signal's underlying carrier. Now, if the code and carrier replicas from this reference channel are used to correlate incoming signals from the other elements, then those channels are code and *frequency* locked (but *not phase locked* due to the net effect of geometry and the array manifold). Phase angles derived from these correlator outputs correspond to the rotation angles needed to phase align the other sample streams to the reference stream (as shown in Figure 3). This procedure is illustrated in **FIGURE 10** for the switched-RF case.

As shown, the 50-Hz databit sign is estimated in the reference channel and used to perform data wipe-off for all channels such that the coherent integration interval can be extended to 1 second. Extending integration time reduces thermal noise and fast-fading multipath.

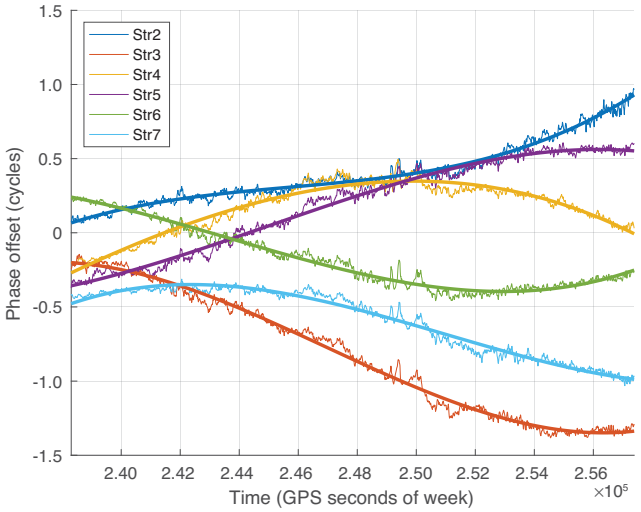

FIGURE 11 Estimated phase offsets for Streams 2 through 7 with respect to center reference element with third-order curve fits.

However, effects of multipath are still present in these 1-Hz phase estimates. Much of this is removed by fitting a third-order polynomial to the data. **FIGURE 11** shows a representative plot of the 1-Hz phase measurements and the fitted polynomials. From these polynomials, phase offsets are computed and applied at a 1-Hz rate for beamforming.

RESULTS

Several hours of sampled data were processed for all satellites in view. Standard receiver outputs such as pseudorange, carrier phase and C/N_0 from all three software receivers (single element, traditional beamforming and correlator beamforming) were recorded, from which multipath mitigation performance results could be derived.

All three software receiver implementations used the same signal tracking parameters at the final measurement-producing state. These steady-state parameters are as follows:

- Carrier loop pre-detection integration time: 20 milliseconds
- PLL order: 3
- PLL noise bandwidth: 18 Hz
- Correlator spacing: 0.1 C/A-code chip
- Code discriminator type: Normalized coherent early-minus-late
- DLL update rate: 10 Hz (performs data wipe-off, as shown in Figure 1)
- DLL noise bandwidth: 1 Hz

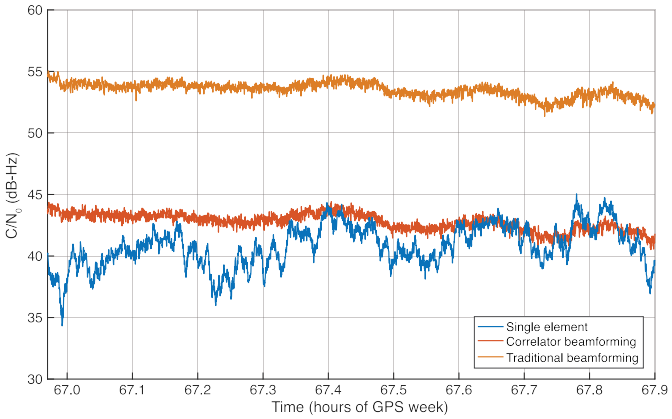

FIGURE 12 C/N_0 measurements over time for PRN06.

- DLL order: 1
- Carrier aiding of code: enabled
- C/N_0 algorithm: narrowband power over wideband power ratio (NBP/WBP)

FIGURE 12 shows representative C/N_0 measurements for satellite PRN06. **TABLE 1** lists the C/N_0 standard deviations for all satellites after de-trending using a second-order curve fit.

For all results obtained, C/N_0 varies significantly for the single-element receiver. This variation is consistent with multipath fading. As expected, multipath fading is nearly absent for the traditional beamforming receiver. This clearly shows how beamforming rejects multipath from off-beam directions. As expected, the $10\log_{10}(7) \approx 8.45$ dB gain advantage of traditional beamforming over correlator beamforming is clearly apparent. Furthermore, C/N_0 of correlator beamforming remains close to that of the center element. However, the most striking result is the multipath

Satellite PRN	Single-element reference	Correlator beamforming	Traditional beamforming
PRN02	2.1	0.44	1.3
PRN05	2.2	0.50	0.82
PRN06	1.5	0.49	0.82
PRN12	2.0	0.41	1.38
PRN19	2.0	0.52	0.80
PRN25	1.5	0.40	0.82

TABLE 1 De-trended C/N_0 standard deviations in dB-Hz.

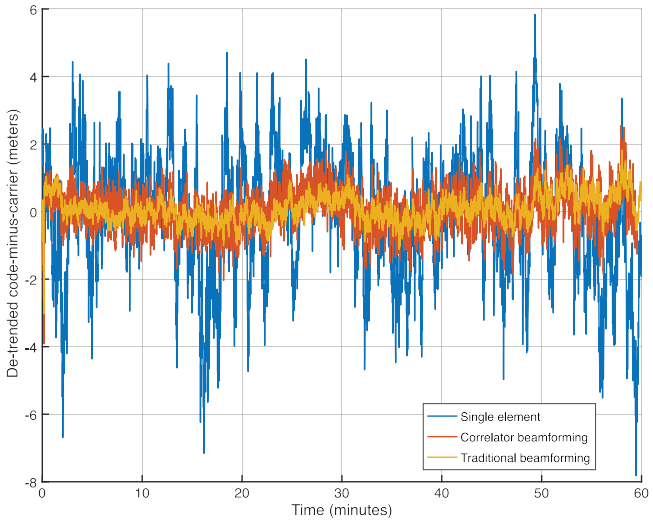

FIGURE 13 De-trended code-minus-carrier for PRN06.

rejection performance of correlator beamforming, as evidenced by the C/N_0 standard deviations.

FIGURE 13 shows representative results for satellite PRN06 for the other characteristic indicator of multipath: code-minus-carrier (CmC) divergence. The de-trended CmC standard deviations for all satellites are summarized in **TABLE 2**. Note that de-trending is used to remove the code-carrier divergence due to the ionosphere.

As shown in Table 2, in terms of CmC divergence, on average, multipath error is reduced by a factor of five for traditional beamforming and almost a factor of four for correlator beamforming.

Finally, the effect of multipath rejection in the position domain was evaluated. **FIGURE 14** shows a horizontal error scatter plot for the three receiver implementations while **FIGURE 15** shows the time series of the individual position components. **TABLE 3** lists the root-mean-square (RMS) position errors and percent error reduction compared

Satellite PRN	Single-element reference	Correlator beamforming	Traditional beamforming
PRN02	4.44	0.66	0.53
PRN06	1.89	0.64	0.41
PRN12	1.12	0.54	0.37
PRN19	2.37	0.77	0.50

TABLE 2 De-trended CmC standard deviations in meters.

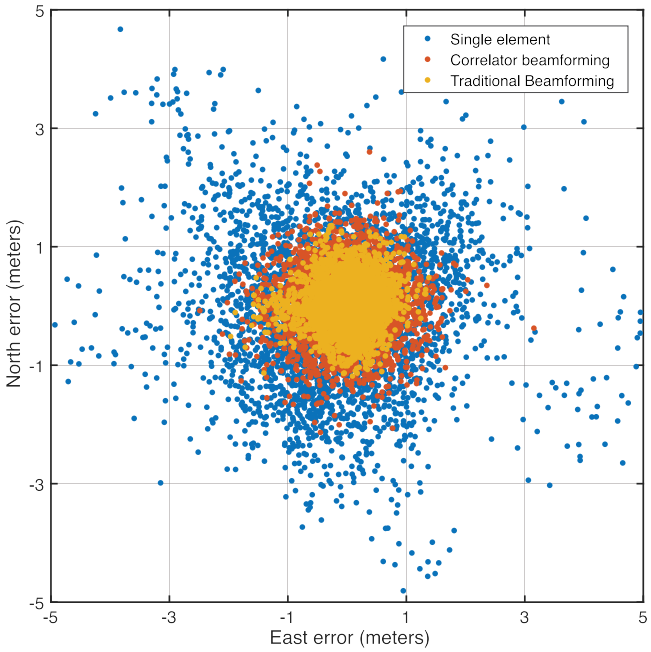

FIGURE 14 Horizontal position error scatter plot for the three receiver implementations.

to the single-element case. On average, traditional beamforming reduces RMS position error by 80 percent compared to a single-element antenna. For correlator beamforming, the average reduction is nearly as good, an impressive 70 percent, but achieved without any of the complexities associated with needing an individual RF front-end for each antenna element. Moreover, the simplified architecture of a correlator beamforming GNSS receiver translates directly into decreased power consumption and reduced size, weight and cost of the resulting antenna electronics unit. Each attribute is highly desirable, especially for portable and personal mobile applications.

CONCLUSIONS

The CRADA effort between AFIT and Locata Corporation took Locata's commercially successful, 2.4-GHz systems and proceeded to investigate the feasibility of applying this new correlator beamforming technology to GNSS receivers. The CRADA focused on demonstrating an easily modified GNSS receiver to potentially deliver a low-cost solution for mitigating multipath — specifically targeting short delay and carrier multipath. The results presented here show that the multipath rejection performance nearly equals that of a traditional beamforming GNSS receiver. Considering the simpler architecture of a correlator

beamforming GNSS receiver, applications that can significantly benefit from this technology include stationary GNSS monitoring installations such as those used in satellite-based and ground-based augmentation systems and GNSS receivers for autonomous vehicles and UAVs in high multipath areas such as urban canyons.

The application of more rigorous calibration techniques will likely improve correlator beamforming performance in a GNSS receiver even further. Moreover, combining this technique with more advanced gated-correlator approaches such as the double-delta correlator could improve multipath mitigation performance further still. The credible advantages that correlator beamforming affords GNSS receivers in terms of size, weight, power and cost and full beamforming-level multipath mitigation performance is worthy of additional investigation and technology development, especially for emerging applications such as autonomous vehicles and UAVs that have a requirement to operate frequently in severe multipath environments such as cities.

DISCLAIMERS

The views expressed in this article are those of the authors and do not reflect the official policy or position of the United States Air Force, Department of Defense, or the United States Government.

ACKNOWLEDGMENTS

This article is based, in part, on the paper "Correlator Beamforming for Multipath Mitigation at Relatively Low Cost: Initial Performance Results" presented at ION GNSS+ 2016, the 29th International Technical Meeting of the Satellite Division of The Institute of Navigation, held Sept. 12–16, 2016, in Portland, Oregon. The authors thank all those who helped and supported the work presented in this article. Specifically, we thank Lt. Col. Phillip Corbell Ph.D. (AFIT professor) for his review and valuable feedback of the correlator beamforming section of this article. We also thank Rick Patton (ANT Center coordinator) for supporting equipment installation and data-collection efforts. The authors would also like to acknowledge and thank Locata Corporation for the excellent support and assistance provided throughout all CRADA activities.

Method	North Error		East Error		Down Error	
	RMS [m]	↓ [%]	RMS [m]	↓ [%]	RMS [m]	↓ [%]
Single-element reference	2.29		1.34		6.41	
Correlator beamforming	0.58	75	0.56	58	1.44	78
Traditional beamforming	0.40	83	0.39	71	0.89	86

TABLE 3 3D RMS position error and percent error reduction with respect to single-element antenna.

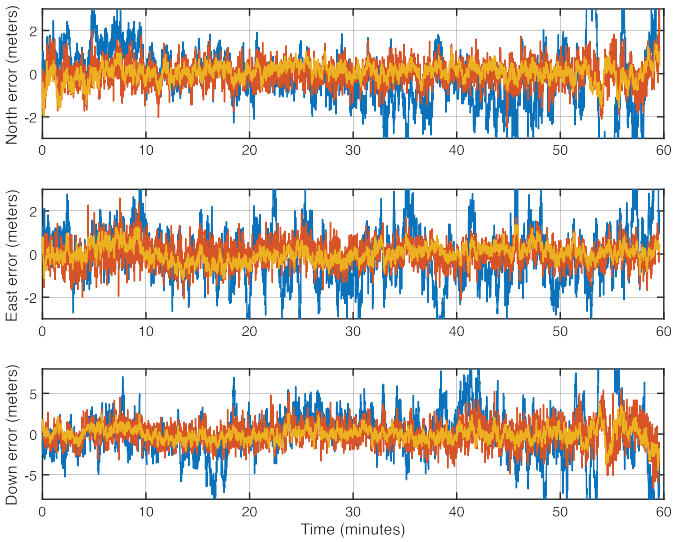

FIGURE 15 3-D position error as a function of time (same color key as Figure 14).

SANJEEV GUNAWARDENA is a research assistant professor of electrical engineering with the Autonomy and Navigation Technology (ANT) Center at the Air Force Institute of Technology (AFIT), Wright-Patterson AFB, Ohio. His research interests include RF design, digital systems design, high-performance computing, software-defined radio (SDR) and all aspects of GNSS receivers and associated signal processing.

JOHN RAQUET is a professor of electrical engineering and the director of the ANT Center at AFIT. He has been involved in navigation-related research for more than 25 years.

MARK CARROLL is a research engineer with AFIT's ANT Center. He received his B.S. and M.S. in computer engineering from Miami University, Oxford, Ohio, in 2012 and 2014, respectively. His current research includes multi-GNSS algorithms, SDRs and other GNSS-related research and development in support of the Air Force Research Laboratory.

MORE ONLINE

Further Reading

For references related to this article, go to **gpsworld.com** and click on "More" in the navigation bar, then on "Innovation."